Available online at www.sciencedirect.com

ScienceDirect

Ceramics International 35 (2009) 2797–2801

CERAMICS INTERNATIONAL

www.elsevier.com/locate/ceramint

Ultraviolet photodetectors based on ZnO nanoparticles

Jin Hyung Jun, Hojun Seong, Kyoungah Cho, Byung-Moo Moon, Sangsig Kim *

Department of Electrical Engineering and Institute for Nano Science, Korea University, Seoul 136-701, Republic of Korea

Received 18 September 2008; received in revised form 7 February 2009; accepted 14 March 2009
Available online 15 April 2009

Abstract

Ultraviolet (UV) photodetectors based on ZnO nanoparticles (NPs) were fabricated and their optoelectronic properties were examined. The dominant photoluminescence (PL) peak of the ZnO NPs was located at a wavelength of 380 nm under the illumination of 325-nm wavelength light. The direct bandgap transition of the charge carriers at λ = 380 nm contributed to the photocurrent. The ratio of the photocurrent to the dark current (on/off ratio) was as high as 10^6, which is favorable for photodetectors. The decay time constant in the photoresponse was relatively small, while the rise time constant was relatively large. The reasons for the high on/off ratio and photoresponse characteristics are discussed in this paper.

Keywords: C. Optoelectrical properties; D. ZnO; Nanoparticles; Photodetectors

1. Introduction

ZnO is one of the n-type semiconducting oxide materials which is widely utilized in the fields of transparent conducting electrodes, varistors, gas sensors and optoelectronic devices [1]. Especially, this oxide material has been extensively studied for its application to the fabrication of ultraviolet (UV) photodetectors, due to its large direct bandgap (~3.3 eV) [2–4]. Photoconduction in ZnO is primarily governed by the adsorption and desorption of oxidizing molecules. In the absence of UV light, oxidizing molecules adsorbed on the surfaces of the oxide materials create electron-depleted layers, which reduce their conductance. When UV irradiation is present, the photogenerated holes move to their surfaces and neutralize the negatively charged oxidizing molecules. This photodesorption process makes their surface conductivity increase significantly. When the UV light is turned off again, the adsorption of oxidizing molecules occurs and the conductivity is reduced again.

Photodetectors with channels made of various types of ZnO have been widely investigated [2,5–9]. Nevertheless, there have been few studies on photodetectors based on zero-dimensional (0-D) ZnO nanoparticles (NPs). The structure of 0-D NPs endows them with better light absorption efficiency than other dimensional structures. Differing from one-dimensional nanowires and two-dimensional quantum well layers, the light absorption characteristics of 0-D NPs are independent of the light polarization [10]. Their superior light absorption characteristics are caused by the enhancement of the excitonic oscillator strength, due to the quantum size confinement effect [11,12], as well as by the concentration of the densities of states near the conduction and valence band edges. When the channel layers of photodetectors are made of NPs, however, some problems related to surface defects still remain. The deep-traps present at the NP surfaces cause rise time delay when the light is illuminated. The chance of irradiative recombination between electrons and holes before charge conduction increases due to these surface defects. Also, the weak resistance of the NPs to chemical substances is another possible problem. In spite of these difficulties related to the surface defects of NPs, a variety of devices based on NPs have been reported [13–16]. One of the most important reasons for developing NP-based devices is that, in addition to the merits originating from their 0-D structure, NPs have the characteristic of solution-processability. In other words, NP-based devices can be fabricated through solution processes. The solution-processability of NPs has some advantages in terms of the ease of fabrication, physical flexibility, large area, and most importantly, low cost.

The basic hypothesis of this study is as follows: if the channel of the photodetector is composed of NPs, the dark

---

* Corresponding author. Tel.: +82 2 3290 3245; fax: +82 2 3290 3894.
E-mail address: sangsig@korea.ac.kr (S. Kim).

0272-8842/$36.00 © 2009 Elsevier Ltd and Techna Group S.r.l. All rights reserved.
doi:10.1016/j.ceramint.2009.03.032

current may be dramatically reduced, due to the numerous junction barriers formed between them. Also, if the number of photogenerated charge carriers significantly increases, the number of charge carriers which jump over the barrier will increase, resulting in an enhancement of the photocurrent and, consequently, in an increase in the ratio of the photocurrent to dark current (the so-called on/off ratio). Since NPs have excellent absorption efficiency, the number of photogenerated charge carriers is maximized and, therefore, the above scenario can be realized. Based on this simple idea, UV photodetectors were fabricated using ZnO NPs as channel materials through the simple painting of the NPs across the pre-patterned electrodes, and their optoelectronic properties were investigated. ZnO NPs with an average size of about 70 nm were used in this work as the channel material, because the exciton Bohr radius of ZnO is estimated to be about 5–50 nm (or 10–100 nm in diameter) [11]. If the NPs are bigger than the exciton Bohr radius, the light is not efficiently absorbed, due to the weak quantum confinement effect, and if the NPs are too small, the transportation of charge carriers through the channel may be difficult, due to the increased scattering probability of the charge carriers at the boundaries of the NPs. Therefore, we chose ZnO NPs with an average diameter of 70 nm, which is in the range of the Bohr radius and not too small in size. After the painting of the ZnO NPs, their photoluminescence (PL) characteristics were examined using the 325 nm wavelength light obtained from a He–Cd laser. The photocurrent response spectrum, photo- and dark-current and photoresponse spectrum taken from the fabricated photodetectors were investigated with a He–Cd laser and a Xe lamp.

2. Experimental

One gram (1 g) of ZnO NPs with an average diameter of about 70 nm (purchased from Sigma–Aldrich Inc.) was dispersed in 20 ml of methanol. The ZnO NPs dispersed in methanol were painted across two gold electrodes with a separation of 20 μm on top of a thermally oxidized Si substrate. The thermal oxide (SiO_2) layer was 300 nm in thickness. The measurements of the PL, photocurrent response spectrum, photocurrent and dark current were performed for the ZnO NPs at room temperature in air. The photoresponses of the ZnO NPs were measured at room temperature at atmospheric pressures of 0.1 atm, 0.5 atm and 1 atm. The light source for these measurements was the 325-nm wavelength line obtained from a He–Cd laser and the optical power of the light source was 3 mW. The excitation source for the photocurrent spectrum was the light from a Xe lamp dispersed by a monochromator.

3. Results and discussion

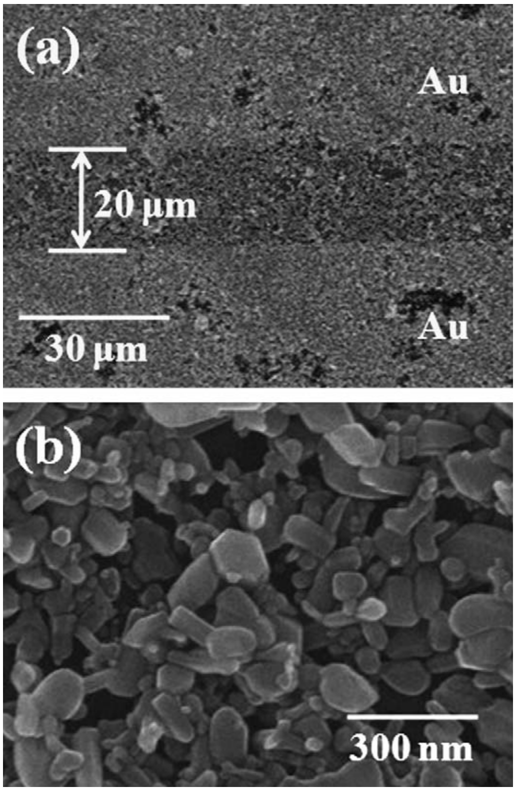

Fig. 1. (a) Low and (b) higher magnification SEM images of the ZnO NPs painted across the gold electrodes.

The SEM image of the ZnO NPs painted across the two gold electrodes with a separation of 20 μm is shown in Fig. 1(a). The SEM image demonstrates that the ZnO NPs are distributed uniformly on the channel region between the electrodes. The higher magnification SEM image of the painted ZnO NPs (Fig. 1(b)) reveals that their size is in the range from 20 nm to 150 nm and that their average size is about 70 nm.

The PL spectrum taken for the ZnO NPs is depicted in Fig. 2. In the PL spectrum, a dominant peak is seen at 380 nm and a broad PL band is centered at 470 nm in the wavelength range from 400 nm to 500 nm. The dominant peak is attributed to the recombination of free excitons through an exciton–exciton collision process [1]. The broad PL band is associated with the electron transition from the level of interstitial Zn to the valence band [17]. In addition, a weak green emission band is present in the wavelength range from 450 nm to 550 nm, and this band originates from oxygen-vacancy-related complexes [18].

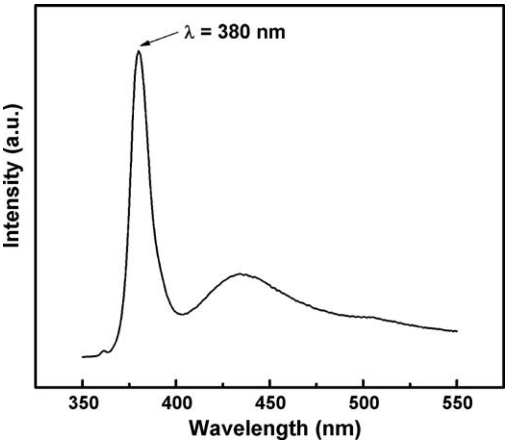

Fig. 2. Photoluminescence spectrum taken for the ZnO NPs using a He–Cd laser with a wavelength of 325 nm.

The photocurrent response spectrum of the ZnO NPs under the modulated illumination of light with continuous wavelengths ranging from 300 nm to 550 nm is presented in Fig. 3. The spectrum represents the above-gap, exciton-related, and below-gap absorption bands for the photocurrents. The above-gap photocurrent mechanism of the ZnO NPs is described first briefly, as follows. When photons with a larger energy than the bandgap energy are incident on the ZnO NPs, electron–hole pairs are generated. The holes generated by the light absorption near the surface neutralize the chemisorbed oxygen, leading to the narrowing of the depletion region of the NPs which results in an increase of the conductivity. The electrons generated at the same time contribute to the increase of the concentration of electrons flowing between the electrodes, thereby increasing the conductivity. Secondly, the sharp peak at a wavelength of 380 nm is in good agreement with the peak of the PL spectrum. The presence of this sharp peak implies that a small fraction of the excitons generated in the NPs by the light absorption contribute to the photocurrent through the dissociation of the excitons. Thirdly, the charge carriers generated by the below-gap light may be trapped at the trap sites in the energy gap. The broad below-gap photocurrent bands in the figure result from this trap mediated hopping of charge carriers in the gap.

The *I*–*V* curves for the photocurrent excited by the 325 nm wavelength light (corresponding to the above-gap absorption) and for the dark current are plotted in Fig. 4. The plot of the dark current is multiplied by 10^5. Both of the *I*–*V* curves show ohmic contact behavior, although the contact of the n-type ZnO and gold electrode would be expected to be Schottky, because of the high work function of ZnO. Their ohmic contact behavior results from the surface impurities and defects of ZnO [19,20]. The plot demonstrates that the photocurrent of the ZnO NPs is 0.3×10^{-6} A in magnitude at 1 V under the 325-nm wavelength light and that the magnitude of the dark current is as low as 0.4×10^{-12} A at 1 V. Consequently, the ratio of the photocurrent to the dark current (on/off ratio) is about 10^6. In addition, the responsivity (R) of the ZnO NP-based photodetector at 1 V was estimated to be 0.1 mA/W according to the following equation:

$$R = \frac{I_{\text{ph}} - I_{\text{dark}}}{P_{\text{op}}}$$

where I_{ph} and I_{dark} are the magnitudes of the photocurrent and dark current, respectively, and P_{op} is the laser power.

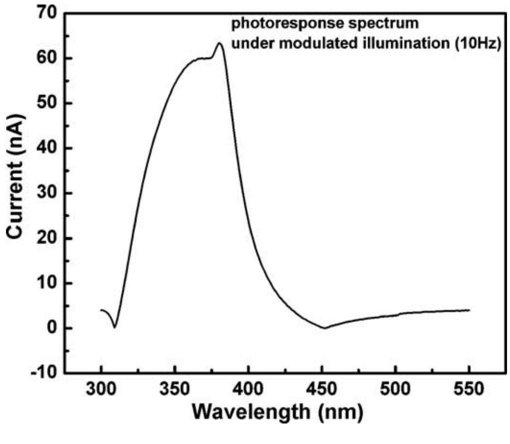

Fig. 3. Photocurrent response spectrum of the ZnO NPs under illumination modulated at a frequency of 10 Hz. The excitation source for the spectrum was the light from a Xe lamp dispersed by a monochromator.

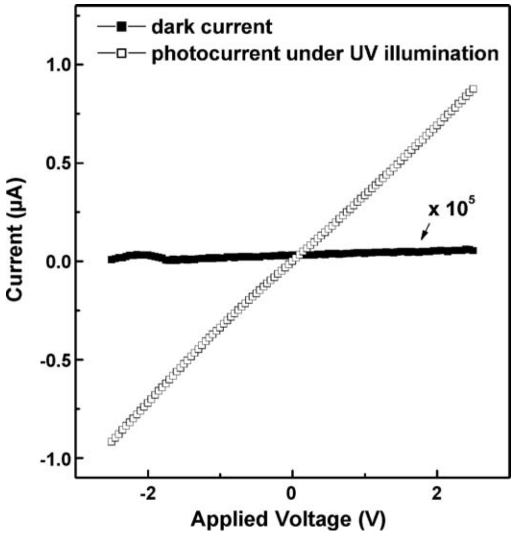

Fig. 4. Dark current and photocurrent of the UV photodetector using the ZnO NPs fabricated in this study. The photocurrent was measured under UV ($\lambda = 325$ nm) illumination and the plots of the dark current were multiplied by 10^5.

Two possible origins for the low magnitude of the dark current are addressed here. The first one is as follows. When the ZnO NPs are exposed to air, the oxidizing gas molecules present in the ambient air are adsorbed on the surfaces of the NPs from which they subsequently capture electrons, resulting in the formation of electron-depleted layers. These electron-depleted layers lower the conductance of the ZnO NPs. The second one is related to the channel structure composed of numerous contacts of ZnO NPs. The junction potential barriers built between the ZnO NPs cause the lowering of the dark current.

The photoresponse of the ZnO NPs measured in ambient air (at an atmospheric pressure of 1 atm) at a bias of 5 V under the periodical illumination of light with a wavelength of 325 nm is plotted in Fig. 5(a). The rise time constant upon illumination was estimated to be $\tau_r = 48$ s. This rise time constant is much larger than those usually observed for the conduction of ZnO bulk (less than a millisecond). The large time constant associated with the rise indicates that the traps in the ZnO NPs are involved in the photocurrent generation process. The photogenerated charge carriers fill the traps and the photocurrent reaches a maximum after all of the traps are filled, which causes a delay in reaching the maximum photocurrent. Due to the significant concentration of traps in the ZnO NPs, the rise time constant is larger than that of ZnO bulk.

After the UV light was switched off, the photocurrent showed rapid decay, following a first order exponential relaxation function with a time constant of $\tau_d = 0.9$ s. This

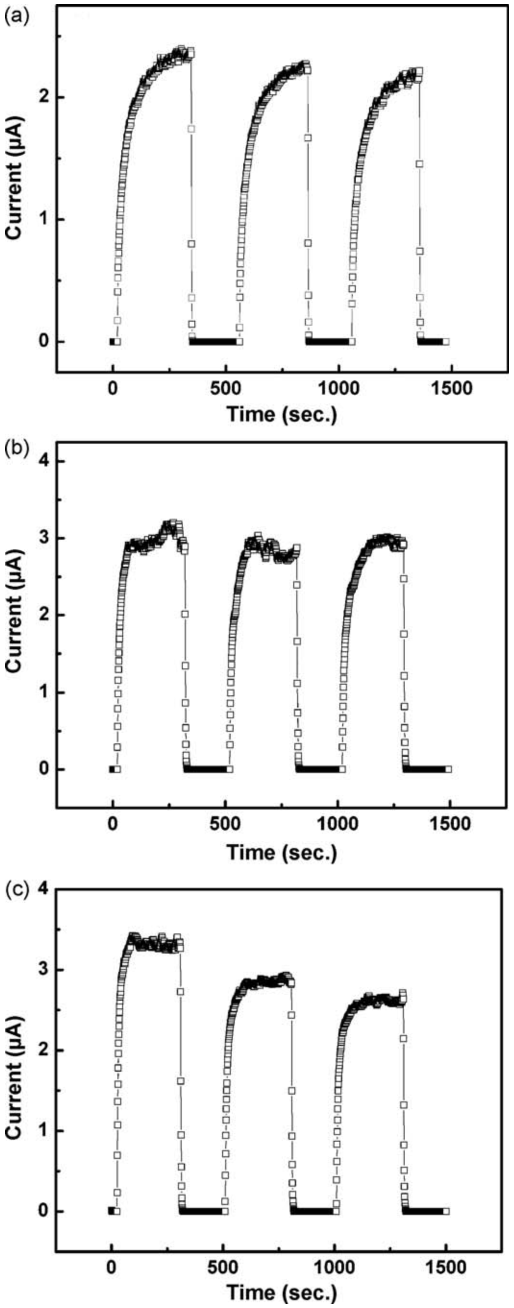

Fig. 5. Plots of the photoresponses of the ZnO-NPs-based UV photodetector at a bias of 5 V under periodical illumination of light with a wavelength of 325 nm. The measurement was performed at (a) 1 atm, (b) 0.5 atm, and (c) 0.1 atm.

value was estimated by the following equation:

$$I = I_0 \, e^{-t/\tau d}$$

where I_0 is the photocurrent under illumination and I is the dark current at elapsed time (t) after switching the light off. Previous studies of photodetectors [9,21,22] reported the existence of a two-step decay mechanism of the photocurrent with a rapid fall in the first step and a slow fall in the second step. In the case of our photodetector, however, the decay of the photocurrent cannot be divided into two steps, because the photocurrent falls rapidly to the initial dark current in just a few seconds. This can be explained by the channel structure of the photodetector using NPs as the channel (sensing) material. When the UV light is switched off, oxidizing molecules are re-adsorbed on the NP surfaces, returning the photodetector to its initial state. The large surface to volume ratio (that is, specific surface area) of the NPs enables immediate re-adsorption of the large amount of oxidizing molecules present on the NP surfaces. Therefore, the photocurrent decays rapidly in the case of our photodetector when the light is turned off.

In order to confirm that the decay of the photodetector is related to the re-adsorption of oxidizing molecules, the photoresponses of the same photodetector were measured at lower atmospheric pressures than 1 atm. The photoresponses measured at pressures of 0.5 atm and 0.1 atm are demonstrated in Fig. 5(b) and (c), respectively. The decay time constant measured at 0.5 atm is about 1.7 s. This value is larger than that measured in ambient air. Also, when the measurement was made at a pressure of 0.1 atm, a larger decay time constant (1.9 s) was obtained. Because the number of gas molecules which can be adsorbed on the NP surfaces (and therefore lower the photocurrent) is less at lower atmospheric pressures, it is reasonable for the decay time constant to become larger. These characteristics clearly prove that the decay of the photocurrent is closely related to the re-adsorption of oxidizing gas molecules. The rise characteristics demonstrated in Fig. 5 also confirm that the adsorption of oxidizing gas molecules is related to the photoresponse. As mentioned above, the rise time constant was 48 s when the photoresponse was measured in air, and the time constant continuously decreased to 30 s and to 13 s as the atmospheric pressure was decreased to 0.5 atm and 0.1 atm, respectively. Since a smaller amount of gas molecules is adsorbed on the NP surfaces at a lower atmospheric pressure, the time required to reach the maximum photocurrent is shortened. Summarizing the rise and decay characteristics in the photoresponses measured at the three selected atmospheric pressures, it can be concluded that the increase and decrease of the magnitude of the photocurrent are governed by the adsorption and re-adsorption of oxidizing gas molecules, respectively.

Although the on–off ratio and responsivity of the NPs-based photodetector fabricated in this study are comparable to those of film-based photodetectors, the NPs-based photodetector showed worse characteristics of decay and rise owing to the surface related defects of the NPs, as compared to film-based photodetectors. Nevertheless, the number of surface defects can be reduced through surface passivation or heat treatment, in order to improve the characteristics of decay and rise in the magnitude of the photocurrent. However, such surface passivation or heat treatment of the NPs will be considered in a future study. Moreover, the compatibility of NPs-based photodetectors with the solution process makes them easier to fabricate and have more physical flexibility, a larger area, and lower cost than film-based photodetectors.

4. Conclusions

UV photodetectors were fabricated using ZnO NPs, and their properties were investigated. A comparison of the PL spectrum and photocurrent response spectrum reveals that a small fraction of the excitons formed under illumination contributes to the photocurrent. The *I–V* characteristics were linear even when measured in the dark. The on/off ratio was 10^6 and the responsivity was 0.1 mA/W at a bias of 1 V. The rise and decay time constants measured in air were estimated to be 48 s and 0.9 s, respectively. In addition, it is confirmed in this study that the increase and decrease in the magnitude of the photocurrent are mainly related to the adsorption and re-adsorption of oxidizing gas molecules, respectively.

Acknowledgments

This work was supported by the National R&D Project for Nano Science and Technology (10022916-2006-22), the Center for Integrated-Nano-Systems (CINS) of the Korea Research Foundation (KRF-2006-005-J03601), the "SystemIC2010" project of the Korea Ministry of Commerce, Industry and Energy, the Korea Science and Engineering Foundation (KOSEF) through the National Research Lab. Program (R0A-2005-000-10045-02 (2007)), and the Nano R&D Program (M10703000980-07M0300-98010).

References

[1] Ü. Özgür, Ya.I. Alivov, C. Liu, A. Teke, M.A. Reshchikov, S. Doğan, V. Avrutin, S.-J. Cho, H. Morkoç, A comprehensive review on ZnO materials and devices, J. Appl. Phys. 98 (4) (2005) 041301.

[2] D.H. Zhang, Fast photoresponse and the related change of crystallite barriers for ZnO films deposited by RF sputtering, J. Phys. D: Appl. Phys. 28 (6) (1995) 1273–1277.

[3] D.C. Look, D.C. Reynolds, J.W. Hemsky, R.L. Jones, J.R. Sizelove, Production and annealing of electron irradiation damage in ZnO, Appl. Phys. Lett. 75 (6) (1999) 811–813.

[4] M. Liu, H.K. Kim, Ultraviolet detection with ultrathin ZnO epitaxial films treated with oxygen plasma, Appl. Phys. Lett. 84 (2) (2004) 173–175.

[5] C.H. Seager, S.M. Myers, Quantitative comparison of dissolved hydrogen density and the electrical and optical properties of ZnO, J. Appl. Phys. 94 (5) (2003) 2888–2894.

[6] J.W. Tomm, B. Ullrich, X.G. Qiu, Y. Segawa, A. Ohtomo, M. Kawasaki, H. Koinuma, Optical and photoelectrical properties of oriented ZnO films, J. Appl. Phys. 87 (4) (2000) 1844–1848.

[7] B.H. Kind, H. Yan, B. Messer, M. Law, P. Yang, Nanowire ultraviolet photodetectors and optical switches, Adv. Mater. 14 (2) (2002) 158–160.

[8] S.S. Hullavarad, N.V. Hullavarad, P.C. Karulkar, A. Luykx, P. Valdivia, Ultra violet sensors based on nanostructured ZnO spheres in network of nanowires: a novel approach, Nanoscale Res. Lett. 2 (3) (2007) 161–167.

[9] S.E. Ahn, J.S. Lee, H. Kim, S. Kim, B.H. Kang, K.H. Kim, G.T. Kim, Photoresponse of sol–gel-synthesized ZnO nanorods, Appl. Phys. Lett. 84 (24) (2004) 5022–5024.

[10] R.T. Senger, K.K. Bajaj, Optical properties of confined polaronic excitons in spherical ionic quantum dots, Phys. Rev. B 68 (4) (2003) 045313.

[11] Y.-N. He, C.-C. Zhu, J.-W. Zhang, The study on mechanism of ultraviolet laser emission at room temperature from nanocrystal thin ZnO films grown on sapphire substrate by L-MBE, Microelectron. J. 35 (4) (2004) 389–392.

[12] Y. Kayanuma, Quantum-size effects of interacting electrons and holes in semiconductor microcrystal with spherical shape, Phys. Rev. B 38 (14) (1988) 9797–9805.

[13] W.U. Huynh, J.J. Dittmer, A.P. Alivisatos, Hybrid nanorod–polymer solar cells, Science 295 (2002) 2424–2427.

[14] H. Sirringhaus, Device physics of solution-processed organic field-effect transitors, Adv. Mater. 17 (2005) 2411–2425.

[15] G. Konstantatos, . Howard, A. Fischer, S. Hoogland, J. Clifford, E. Klem, L. Levina, E.H. Sargent, Ultrasensitive solution-cast quantum dot photodetectors, Nature 442 (2006) 180–183.

[16] Y. Sun, J.A. Rogers, Inorganic semiconductors for flexible electronics, Adv. Mater. 19 (2007) 1897–1916.

[17] Z. Fang, Y. Wang, D. Xu, Y. Tan, X. Liu, Blue luminescent center in ZnO films deposited on silicon substrates, Opt. Mater. 26 (3) (2004) 239–242.

[18] F.K. Shan, G.X. Liu, W.J. Lee, G.H. Lee, I.S. Kim, B.C. Shin, Aging effect and origin of deep-level emission in ZnO thin film deposited by pulsed laser deposition, Appl. Phys. Lett. 86 (22) (2005) 221910.

[19] S. Liang, H. Sheng, Y. Liu, Z. Huo, Y. Lu, H. Shen, ZnO Schottky ultraviolet photodetectors, J. Cryst. Growth 225 (2–4) (2001) 110–113.

[20] B.J. Coppa, C.C. Fulton, S.M. Kiesel, R.F. Davis, C. Pandarinath, J.E. Burnette, R.J. Nemanich, D.J. Smith, Structural, microstructural, and electrical properties of gold films and Schottky contacts on remote plasma-cleaned, n-type ZnO{0 0 0 1} surfaces, J. Appl. Phys. 97 (10) (2005) 103517.

[21] K.W. Liu, J.G. Ma, J.Y. Zhang, Y.M. Lu, D.Y. Jiang, B.H. Li, D.X. Zhao, Z.Z. Zhang, B. Yao, D.Z. Shen, Ultraviolet photoconductive detector with high visible rejection and fast photoresponse based on ZnO thin film, Solid-State Electron. 51 (5) (2007) 757–761.

[22] Y. Jiang, W.J. Zhang, J.S. Jie, X.M. Meng, X. Fan, S.-T. Lee, Photoresponse properties of CdSe single-nanoribbon photodetectors, Adv. Funct. Mater. 17 (11) (2007) 1795–1800.